

Testing the Copernican principle by constraining spatial homogeneity

Wessel Valkenburg¹, Valerio Marra² and Chris Clarkson³

¹*Instituut-Lorentz for Theoretical Physics, Universiteit Leiden, Postbus 9506, 2333 CA Leiden, The Netherlands*

²*Institut für Theoretische Physik, Universität Heidelberg, Philosophenweg 16, 69120 Heidelberg, Germany*

³*Astrophysics, Cosmology and Gravity Centre, and Department of Mathematics and Applied Mathematics, University of Cape Town, Rondebosch 7701, South Africa*

Accepted XXX. Received XXX; in original form XXX

ABSTRACT

We present a new programme for placing constraints on radial inhomogeneity in a dark-energy dominated universe. We introduce a new measure to quantify violations of the Copernican principle. Any violation of this principle would interfere with our interpretation of any dark-energy evolution. In particular, we find that current observations place reasonably tight constraints on possible late-time violations of the Copernican principle: the allowed area in the parameter space of amplitude and scale of a spherical inhomogeneity around the observer has to be reduced by a factor of three so as to confirm the Copernican principle. Then, by marginalizing over possible radial inhomogeneity we provide the first constraints on the cosmological constant which are free of the homogeneity prior prevalent in cosmology.

Key words: Dark energy, large-scale structure of the Universe, Copernican principle

1 INTRODUCTION

The Copernican principle states that humans are not privileged observers of the universe and provides our philosophical basis for assuming that on the largest scales the universe is spatially homogeneous. While it is one of the foundational aspects of modern cosmology, this assumption needs to be tested outside of the standard paradigm (Bolejko & Wyithe 2009; Davis et al. 2011; Valkenburg 2012b; Marra et al. 2013). Though it may seem pedantic to test something so obvious, the standard paradigm itself is built on shaky foundations, relying on an unexplained, gravitationally repulsive, dark-energy component for observations to fit the model. As current observations suggest isotropy around us (Blomqvist & Mortsell 2010; Komatsu et al. 2011), inhomogeneous models must have the observer near the centre of a matter distribution which is approximately spherically symmetric. Because we can observe changes in the expansion of the universe as a function of redshift only, it remains hard to disentangle temporal evolution from possible spatial variations spherically around us. Indeed, there has even been active debate on models whereby dark energy is replaced by radial inhomogeneity, in violation of the Copernican principle (see Marra & Notari 2011; Clarkson 2012 for reviews). This highlights how intertwined are attempts to detect any evolution of dark energy to the Copernican principle.

To rule out spherically symmetric models, consistency tests have been proposed (see Clarkson 2012 for a review), but all suffer as they lack at present a quantifiable measure of

deviations from homogeneity. Attempts have been made to measure the homogeneity of the universe (Hogg et al. 2005; Labini & Baryshev 2010; Scrimgeour et al. 2012; Jackson 2012; Marinoni et al. 2012; Keenan et al. 2013). Here we introduce a robust approach, by directly constraining any radial change in the density, Hubble rate and curvature assuming that the Copernican principle is *false* and that dark energy exists. We model the universe spherically symmetric, containing both matter and dark energy in the form of a cosmological constant. We provide marginalized constraints on the amplitude and scale of any spatial inhomogeneity. We quantify the deviation from Copernicanism by comparing the observational constraints we find on the spherical inhomogeneity to the theoretical constraints on the existence of the same inhomogeneity in a Copernican universe. The ratio of allowed volumes in parameter space describing the inhomogeneity gives a measure of how far we are from establishing the Copernican principle. Our goal is not to extend the Λ CDM model, but to find how ‘badly’ non-Copernican a feature the model can have. Occam’s razor already favours the Copernican Universe. But Occam’s razor is a model selection tool. Here, we lay out a programme to *falsify* non-Copernican models, so as to establish the Copernican Principle observationally.

2 THE MODEL

We model radial inhomogeneity assuming a spherically symmetric Lemaître-Tolman-Bondi solution including a cosmological constant Λ (ALTb), see e.g. (Lemaitre 1997; Tolman 1934; Bondi 1947; Romano et al. 2012; Sinclair et al. 2010; Marra & Paakkonen 2010; Valkenburg 2012a). The metric is given by

$$ds^2 = -dt^2 + \frac{a_{\parallel}^2(t, r)}{1 - k(r)r^2} dr^2 + a_{\perp}^2(t, r) r^2 d\Omega^2, \quad (1)$$

where the radial (a_{\parallel}) and angular (a_{\perp}) scale factors are related by $a_{\parallel} = (a_{\perp} r)'$. A prime denotes partial derivation with respect to the coordinate radius r . The curvature $k = k(r)$ is a free function. The Friedmann-Lemaître-Robertson-Walker (FLRW) limit is $k \rightarrow \text{const.}$, and $a_{\perp} = a_{\parallel}$. The two scale factors define two Hubble rates:

$$H_{\perp} = H_{\perp}(t, r) \equiv \dot{a}_{\perp}/a_{\perp}, \quad H_{\parallel} = H_{\parallel}(t, r) \equiv \dot{a}_{\parallel}/a_{\parallel}. \quad (2)$$

The analogue of the Friedmann equation in this space-time is then given by $H_{\perp}^2 = m(r)/a_{\perp}^3 - k/a_{\perp}^2 + \Lambda/3$, where $m(r)$ is a non-negative free function of r related to the locally measured matter density $8\pi G \rho_m(t, r) = (m(r)r^3)' / a_{\parallel} a_{\perp}^2 r^2$, which obeys the conservation equation $\rho_m' + (2H_{\perp} + H_{\parallel})\rho_m = 0$. Dimensionless density parameters for the CDM and curvature are in analogy with the FLRW models:

$$\Omega_m(r) = \frac{m}{H_{\perp}^2 a_{\perp}^3}, \quad \Omega_k(r) = -\frac{k}{H_{\perp}^2 a_{\perp}^2}, \quad \Omega_{\Lambda}(r) = \frac{\Lambda}{3H_{\perp}^2}, \quad (3)$$

so that $\Omega_m(r) + \Omega_k(r) + \Omega_{\Lambda}(r) = 1$. Note that in the previous equation the gauge fixing $a_{\perp}(t_0, r) = 1$ has been used. Moreover, Ω_{Λ} depends on r because the present-day expansion rate $H_{\perp 0}$ is inhomogeneous. Using (3) the Friedmann equation takes on its familiar form: $H_{\perp}^2/H_{\perp 0}^2 = \Omega_m a_{\perp}^{-3} + \Omega_k a_{\perp}^{-2} + \Omega_{\Lambda}$. Integrating the Friedmann equation from the time of the big bang $t_{\text{bb}}(r)$ to some later time t yields the age of the universe at a given (t, r) : $t - t_{\text{bb}} = \frac{1}{H_{\perp 0}(r)} \int_0^{a_{\perp}(t, r)} \frac{dx}{\sqrt{\Omega_m(r)x^{-1} + \Omega_k(r) + \Omega_{\Lambda}(r)x^2}}$. Hence there is a relation between the functions t_{bb} , Ω_k and Ω_m . Therefore the ALTb model is specified by two free functional degrees of freedom, and we use $\Omega_k(r)$ and $t_{\text{bb}}(r)$. By demanding a homogeneous age of the universe we fix the bang function to zero, $t_{\text{bb}}(r) = 0$. This ensures the absence of decaying modes in the matter density (Silk 1977; Zibin 2008), in agreement with the standard inflationary scenario.

We parametrize the only left freedom with the curvature function with the monotonic profile

$$k_{\alpha}(r) = k_b + (k_c - k_b) P_3(r/r_b, \alpha), \quad (4)$$

where r_b is the comoving radius of the spherical inhomogeneity and the function $P_n - C^n$ everywhere – is:

$$P_n(x, \alpha) = \begin{cases} 1 & \text{for } 0 \leq x < \alpha \\ 1 - e^{-\frac{1-\alpha}{x-\alpha}(1-\frac{x-\alpha}{1-\alpha})^n} & \text{for } \alpha \leq x < 1 \\ 0 & \text{for } x \geq 1 \end{cases} \quad (5)$$

We choose $n = 3$, such that the metric is C^2 and the Riemann curvature is C^0 . Moreover, for $r \geq r_b$ the curvature profile equals k_b such that there the metric describes *exactly* a curved Λ CDM model (α parametrizes the transition $k_c \rightarrow k_b$). The central over- or under-density, determined by

curvature k_c , is automatically compensated by a surrounding under- or over-dense shell. Hence r_b , k_c and α are the free parameters relative to the non-Copernican feature.

Finally, on the past light cone of a central observer, $t(z)$ and $r(z)$ are determined as a function of redshift z by the differential equations for radial null geodesics, $\frac{dt}{dz} = \frac{-1}{(1+z)H_{\parallel}}$

and $\frac{dr}{dz} = \frac{\sqrt{1-k(r)^2}}{(1+z)a_{\parallel}H_{\parallel}}$, where H_{\parallel} and a_{\parallel} are evaluated on the light cone. The area (d_A) and luminosity (d_L) distances are given by $d_A(z) = a_{\perp}(t(z), r(z)) r(z)$, $d_L = (1+z)^2 d_A$.

3 DATA & OBSERVABLES

H₀: The local Hubble rate is obtained by measuring cosmological standard candles mostly within a redshift range $z_{\text{min}} \leq z \leq z_{\text{max}}$ which depends on the redshift volume that is probed by a given experiment. We compare the observed value to the theoretical quantity,

$$H_0 = \frac{c(z_{\text{max}} - z_{\text{min}})}{\int_{z_{\text{min}}}^{z_{\text{max}}} d_L(z)/[z + \frac{1}{2}(1-q_0)z^2] dz}, \quad (6)$$

where the deceleration parameter at the centre $q_0 = \Omega_m(0)/2 - \Omega_{\Lambda}(0)$ is used to expand the luminosity distance to the second order in redshift. The reason we compare an averaged expansion rate to the data is because the observed H_0 in fact comes from averaging distances, so this should be a fair comparison. We use the value measured by Riess et al. (2011) of $H_{\text{Riess}} = 73.8 \pm 2.4 \text{ km s}^{-1} \text{ Mpc}^{-1}$, with $z_{\text{min}} = 0.01$ and $z_{\text{max}} = 0.1$. One could be tempted to say that modern cosmic-microwave-background (CMB) data constrain H_0 already sufficiently without the inclusion of the astrophysical data that we discuss here. However, it is crucial to realise that *only in a purely homogeneous universe*, these two measurements measure the same quantity. When considering the non-Copernican feature at hand, the expansion rate varies spatially and hence a model can predict different values for the local astrophysical H_0 (local expansion rate) and the CMB H_0 (the age of the universe and inferred from it the global expansion rate today).

Supernovae Ia: We use the SNLS3 catalogue (Guy et al. 2010), which consists of 472 type Ia supernovae in the redshift range $z = 0.01 - 1.39$. We include two nuisance parameters describing stretch-luminosity and colour-luminosity relationships, as in Guy et al. (2010).

CMB: We fit the CMB according to the method presented in Moss et al. (2011); Biswas et al. (2010), in which an effective FLRW metric is used to account for the different area distance to the surface of last scattering as compared to the homogeneous background model. This method ignores isocurvature modes (consistent with the choice of a homogeneous big bang), assumes a standard number of relativistic degrees of freedom and a standard power spectrum, all of which would change the constraints (Clarkson 2012). Moreover, we assume that the late-time integrated Sachs-Wolfe effect is not affected by the presence of the inhomogeneity, as the latter will turn out to be of a magnitude such that it can be described as linear perturbations on an FLRW metric (see the discussion below about the kSZ observable). We fit our model to WMAP 7-year data (Komatsu et al. 2011).

Baryon Acoustic Oscillations (BAO): The sound horizon at the time of the drag epoch t_d is imprinted in the

galaxy correlation function. In a spherically symmetric inhomogeneous model this is an ellipsoid with proper scales, when viewed from the centre

$$L_{\perp}(z) = d_s a_{\perp}(z)/a_{\perp}(t_d, r(z)) = d_A(z) \theta_s(z), \quad (7)$$

$$L_{\parallel}(z) = d_s a_{\parallel}(z)/a_{\parallel}(t_d, r(z)) = z_s(z)/[(1+z)H_{\parallel}(z)], \quad (8)$$

where θ_s is the angle that the acoustic scale subtends on the sky, and z_s is the redshift interval corresponding to the acoustic scale in the radial direction. The sound horizon d_s is calculated assuming a homogeneous early universe. We use observations from SDSS, 6DFGS and WiggleZ (Percival et al. 2010; Beutler et al. 2011; Blake et al. 2011), as compiled in Zumalacarre et al. (2012).

Compton y -distortion: Off-centre observers see a large dipole in the CMB in an inhomogeneous universe. CMB photons are scattered from inside our past light-cone into our line-of-sight by off-centre reionized structures which act as mirrors. The spectrum observed by the central observer is then a mixture of blackbody spectra with different temperatures, producing a distorted blackbody spectrum. In the single-scattering and linear approximations, and when the temperature anisotropy is dominated by the induced dipole β , the y -distortion can be written as (Moss et al. 2011):

$$y = \frac{7}{10} \int_0^{r_{\text{re}}} dr \frac{d\tau}{dr} \beta(r)^2, \quad (9)$$

where r is the comoving distance down the light cone and r_{re} marks the reionization epoch. The time dependence of the optical depth is given by $d\tau/dt = \sigma_T n_e(t) = \sigma_T f_b (1 - Y_{\text{He}}/2) \rho_m(t)/m_p$, where σ_T is the Thomson cross-section, $f_b \equiv \rho_b/\rho_m$ is the baryon fraction, Y_{He} is the helium mass fraction and m_p is the proton mass. The dipole β is found by integrating the geodesic equations in the negative and positive r -directions starting from an observer at $\{t(z), r(z)\}$ back to the surface of last scattering. The difference in redshift between the two directions is then approximately translated into the dipole observed by the scatterer: $\beta = (z_+ - z_-)/(2 + z_+ + z_-)$. The 2σ upper limit from the COBE satellite (Fixsen et al. 1996) is $y < 1.5 \times 10^{-5}$.

kSZ: The dipole β affects the observed CMB also through the kinetic Sunyaev-Zel'dovich (kSZ) effect (Garcia-Bellido & Haugboelle 2008): hot electrons inside an overdensity distort the CMB spectrum through inverse Compton scattering, in which low energy CMB photons receive energy boosts during collisions with the high-energy electrons. Here we focus on the ‘linear kSZ effect’ (Zhang & Stebbins 2011), in which the effect due to all free electrons in the reionized universe is taken into account. Using the Limber approximation, the kSZ power at multipole ℓ is given by (Zibin & Moss 2011): $C_{\ell}^{\text{kSZ}} \simeq \frac{16\pi^2}{(2\ell+1)^3} \int_0^{r_{\text{re}}} dr r [\beta(r) \frac{d\tau}{dr}]^2 \Delta_m^2(\hat{k}(r), r)$, where $\Delta_m^2(k, z) = \frac{k^3}{2\pi^2} P_m(k, z)$ is the dimensionless power spectrum of the background model and the function $\hat{k}(r) \equiv \hat{k}(k(r), z(r))$ is necessary to ‘isotropize’ the angular and radial wave numbers which in an inhomogeneous universe evolve differently: $\hat{k}(\bar{k}, z) = \bar{k}[(1 + \bar{z})a_{\perp}(\bar{t}, r(z))^{2/3}a_{\parallel}(\bar{t}, r(z))^{1/3}]/[(1+z)a_{\perp}(z)^{2/3}a_{\parallel}(z)^{1/3}]$. We constrain inhomogeneous models using a top hat prior $0 < l(l+1) [C_{\ell=3000}^{\text{TT}} + C_{\ell=3000}^{\text{kSZ}}] < 59 \mu\text{K}^2$, based on the results from SPT (Shirokoff et al. 2011).

As we will see in the results, the use of a matter power

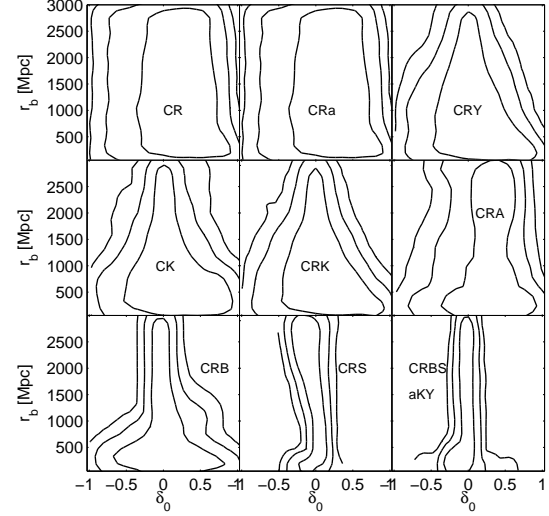


Figure 1. Marginalized constraints on r_b and δ_0 from different combinations of data: ‘C’ refers to CMB, ‘R’ to H_0 , ‘B’ to BAO, ‘S’ to SN, ‘A’ to absolute age data, ‘a’ to age data used as lower bound only, ‘K’ to kSZ, ‘Y’ to Compton- y distortion. The strongest constraints at low redshifts come from SN, while the strongest constraint on δ_0 on large scales seems to come from kSZ. Naturally all data sets combined give the strongest constraints.

spectrum that is computed in the FLRW metric, $\Delta_m^2(k, z)$, even though the correct metric is the LTB metric, is justified. Density contrasts that we encounter in the LTB metric are of magnitudes such that they could be described as a linear perturbation on the FLRW metric. Therefore, any deviation of $\Delta_m^2(k, z)$ from its FLRW evolution as a consequence of the spherical perturbation, is of second order in perturbation theory and hence suppressed since both $\Delta_m^2(k, z)$ and the spherical perturbation are at the linear level. This argument may sound contradictory to the findings of Nishikawa et al. (2012). However, in Nishikawa et al. (2012) it is found that structures with a central density $\delta_0 = -1$ and radius $L = 12\text{Gpc}$ have a radius-dependent growth factor significantly different from FLRW. Such structures can clearly not be considered a linear perturbation ($|\delta| \sim 1$) and one cannot expect that superposed perturbations continue to behave uncoupled (linearly). In the scenario at hand, the assumption that perturbations remain linear, and hence that an FLRW $P(k)$ superposed on a linear LTB perturbation grows effectively as in pure FLRW, is justified.

Age data: Finally, we constrain radial inhomogeneity also by means of galaxy ages (Bolejko et al. 2011; McCarthy et al. 2004; Simon et al. 2005; Stern et al. 2010; Moresco et al. 2012; Wang & Zhang 2012; de Putter et al. 2013). In particular, we use the cosmology independent age vs. redshift data as compiled in de Putter et al. (2013), which in the most conservative approach only provides a lower bound on cosmic ages. For completeness we present results using these ages as lower bounds as well as using them as absolute age measurements (see de Putter et al. 2013 for details).

4 COPERNICAN PRIOR

Given a Gaussian density field, the mean square of density perturbations inside a sphere of radius L around any point (hence also around the observer) today is given by $\sigma_L^2 = \int_0^\infty \frac{dk}{k} \Delta_{m0}^2(k) [3j_1(Lk)/Lk]^2$, where Δ_{m0} is the power spectrum today inferred from the CMB temperature spectrum, assuming a Copernican universe, and j_l is the spherical Bessel function of the first kind. We calculate σ_L for the radius $L < r_b$ at which the central over-/under-density makes the transition to the surrounding mass-compensating under-/over-dense shell. Then we compute the actual density perturbation $\delta_0 \equiv M(L)/\bar{M}(L) - 1$ of a given inhomogeneity and define the Copernican prior as the probability

$$P(\delta_0, L) = (\sigma_L \sqrt{2\pi})^{-1} \exp \left[-\frac{1}{2} (\delta_0 / \sigma_L)^2 \right], \quad (10)$$

where $M(r) \equiv 4\pi \int_0^r dr' \sqrt{-g} \rho_m(r')$ is the mass of the inhomogeneity, $\bar{M}(r) = M(r)|_{k(r)=k_b}$ is the mass relative to the background, and g the determinant of the metric (1). A similar function has been used by [Hunt & Sarkar \(2010\)](#) to compute the probability of having a large void in an Einstein-de Sitter universe, so large that the need for a cosmological constant vanishes (which is not the case considered here).

5 ANALYSIS

We explore a 14-dimensional parameter space using CosmoMC ([Lewis & Bridle 2002](#)): three parameters describing the inhomogeneity, an overall curvature term, the ratio of baryons to dark matter, the cosmological constant, the optical depth to the last scattering surface, the age of the universe, three spectral parameters for the CMB (scalar amplitude, tilt and running of the tilt), the amplitude of a thermal SZ template that is used for the CMB spectrum and the two SN nuisance parameters. We calculate cosmic distances using VOIDDISTANCESII ([Marra et al. 2013](#)), and compute the corrected CMB spectrum using CAMB ([Lewis et al. 2000](#)).

Given the curvature parameter k_c that describes the spherical patch, in Eq. (4), we compute the density contrast δ_0 as the ratio of the determinant of the metric (1) at $r = 0$ and $r > r_b$, since the coordinates are synchronous and comoving. In fact, we take a flat prior on the central density contrast $-1 < \delta_0 < 1$, and obtain the actual curvature parameters in each step of the Monte Carlo Markov Chain (MCMC) by numerical inversion. Fundamentally, δ_0 is mathematically not constrained from above, such that our prior looks artificially constraining. As we will see however, the observations favour $\delta_0 < 1$, such that we can safely state that our result is prior independent. Also, we take a flat prior on r_b and α on the ranges $50\text{Mpc} < r_b < 3000\text{Mpc}$ and $0 < \alpha < 1$. There is a slight degeneracy between r_b and α , as a smoother transition (smaller α) and larger radius give the same difference in gravitational potential at the centre and outside of the feature. However – as can be seen by comparing Fig. 2 to the lower right panel in Fig. 1 – constraints on L do not differ qualitatively from constraints on r_b , while the relation between r_b and L depends on α . This implies that the degeneracy does not significantly bias the results.

We will consider all previously discussed observables in conjunction with CMB and H_0 data. The reason for this is

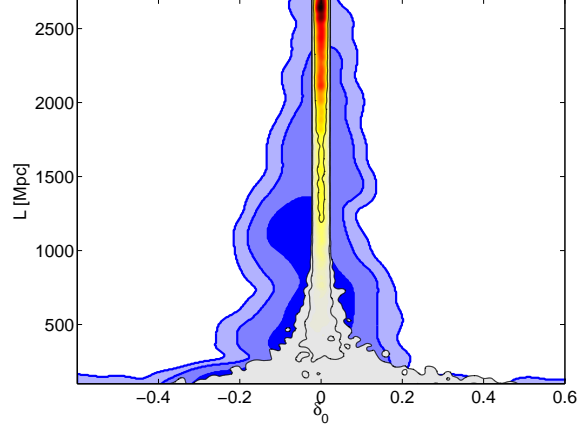


Figure 2. Marginalized posterior probability of L and δ_0 from all data sets combined (blue contours, closely related to CRBSaKY (CMB, H_0 , BAO, SN, age data, kSZ and Compton- y) in Fig. 1, albeit with a slightly different quantity on the vertical axis) at 68%, 95% and 99% confidence level (c.l.), compared to the Copernican prior obtained by fitting CMB only while imposing the Copernican prior, (red to gray colouring) at 68%, 95% and 99% c.l. The ratio of the areas of the 99%-c.l. surfaces is roughly a factor of three. The allowed area needs to be reduced by a factor of three so as to confirm the Copernican principle. The marginalized 95% c.l. limits on the contrast are $-0.29 < \delta_0 < 0.14$ for CRBSaKY and $-0.12 < \delta_0 < 0.12$ for the Copernican prior.

that in all cases we use the same set of 11 (Λ CDM) + 3 (non-Copernican feature) parameters and we wish not to bias the constraining power of any data set by fixing any parameter that at first sight might seem unrelated. At the same time, none of the individual data sets can constrain all 14 parameters all by itself, which explains the need for the inclusion of the CMB and H_0 . Moreover, the kSZ and Compton- y effects depend directly on the CMB data, such that it would not make sense to consider them without computing the CMB power spectrum. The kSZ effect is nothing but an alteration of the CMB power spectrum, while the Compton- y effect depends on the spectral distortions, which do not enter the power spectrum. That is, no data is double counted. In summary, we do not want to fix any parameter, but having many parameters completely unconstrained is inconvenient for the MCMC analysis and hence we always include CMB and H_0 .

6 RESULTS

We present our results in terms of the non-Copernican parameters δ_0 and r_b , marginalizing over all other aforementioned parameters. In Fig. 1 we show the constraints on the non-Copernican parameters from a number of possible combinations of data sets, ordered by constraining power. In all cases we use the CMB constraints in combination with at least one other data set. Not surprisingly, all data sets combined provide the strongest constraints, only allowing for a narrow range of contrasts, however for many radii. As warned for in the introduction, none of the observables actually favors $\delta_0 \neq 0$. But as argued, the purpose of this Letter is not to establish the Copernican principle, but instead to falsify the extra parameters observationally.

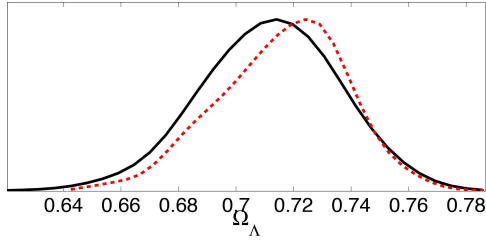


Figure 3. Marginalized posterior probability for Ω_Λ when ignoring inhomogeneity (red dashed line), $\Omega_\Lambda = 0.71 \pm 0.05$ at 95% c.l., and when including inhomogeneity and marginalizing over it (solid black line), $\Omega_\Lambda = 0.76 \pm 0.05$ at 95% c.l. Both constraints correspond to the CRBSaKY observables, see Fig. 1.

The first panel shows that the combination of CMB and H_0 data is hardly constraining on the radius of the non-Copernican feature, and only mildly on the central density. This can be understood by realizing that the central expansion rate is linearly related to the central density contrast, and not at all to the radius, while the CMB is only a standard candle at very high redshift, which does almost not depend on the non-Copernican feature. The third, fourth and fifth panels isolate the constraining power from the kSZ effect and Compton-y distortion. Both these effects depend on the anisotropy of the CMB at outer radii, which is to first approximation sensitive to the depth of the gravitational potential of the non-Copernican feature. Keeping the density contrast constant, but increasing the radius, will increase the depth of the potential. Indeed, these observables constrain mostly the larger radii. The age data used as a lower bound hardly constrain the inhomogeneity, while the absolute data which have both an upper and a lower bound merely serve as an illustration, as these cannot be used in the LTB metric (de Putter et al. 2013). At last, the observables CMB, H_0 , BAO and SNe are a set that for this analysis is an angular diameter distance measurement at many redshifts. As such, the SNe are most strongly constraining at small radii, because a large value of δ_0 at these radii cannot transit back to zero sufficiently quickly without predicting a bump in the luminosity distance that violates SN observations.

The key result of this Letter is shown in Fig. 2, where we compare the posterior probability from all data sets to a posterior which is the Copernican prior convolved with the CMB likelihood, $\tilde{P}(\delta_0, L) = \int dp_i P(\delta_0, L) \mathcal{L}_{\text{CMB}}(p_i, \delta_0, L)$, where p_i denote *all* parameters other than δ_0 and L , and $\mathcal{L}_{\text{CMB}}(p_i, \delta_0, L)$ is the likelihood of the CMB data given the model and its parameters p_i , δ_0 and L . In words, \tilde{P} is the probability distribution of δ_0 and L , given the matter power spectrum obtained from the CMB and its uncertainty, which under the Copernican principle is the power spectrum around us. We find that the area of constraints on L and δ_0 needs to decrease by a factor of three to confirm the Copernican principle, because then observations on the lightcone constrain inhomogeneity to within the range allowed for by the CMB power spectrum. Finally, in Fig. 3 we show for the first time constraints on the cosmological constant, Λ , marginalized over the effect of inhomogeneities around us, compared to the same constraints without taking into account inhomogeneity. We find that error bars increase by 15% if one marginalizes over inhomogeneity.

The analysis regarding the constraints from H_0 , SNe, BAO and kSZ uses data and results that have been obtained assuming, at some point, an FLRW framework. While we correctly used the processed data so as to compare it with the inhomogeneous universe, in principle one should confront to data that are as close to raw as possible. While this caveat should be kept in mind, we do not expect the analysis to be sizeably biased because the inhomogeneous universe we are considering does not depart strongly from its FLRW background, as shown by the results of Fig. 2. Our constraints apply to inhomogeneity which arise at late times, and do not apply to non-Copernican properties at early times. We assumed that dark energy is described by a cosmological constant and that general relativity is the correct theory of gravity.

ACKNOWLEDGEMENTS

WV is supported by a Veni research grant from the Netherlands Organisation for Scientific Research (NWO).

REFERENCES

- Beutler F., Blake C., Colless M., Jones D. H., Staveley-Smith L., et al., 2011, *Mon.Not.Roy.Astron.Soc.*, 416, 3017
- Biswas T., Notari A., Valkenburg W., 2010, *JCAP*, 1011, 030
- Blake C., Kazin E., Beutler F., Davis T., Parkinson D., et al., 2011, *Mon.Not.Roy.Astron.Soc.*, 418, 1707
- Blomqvist M., Mortsell E., 2010, *JCAP*, 1005, 006
- Bolejko K., Hellaby C., Alfedeel A. H. A., 2011, *JCAP*, 1109, 011
- Bolejko K., Wyithe J. S. B., 2009, *JCAP*, 0902, 020
- Bondi H., 1947, *Mon.Not.Roy.Astron.Soc.*, 107, 410
- Clarkson C., 2012, *Comptes Rendus Physique*, 13, 682
- Davis T. M., Hui L., Frieman J. A., Haugbolle T., Kessler R., et al., 2011, *Astrophys.J.*, 741, 67
- de Putter R., Verde L., Jimenez R., 2013, *JCAP*, 1302, 047
- Fixsen D. J., et al., 1996, *Astrophys. J.*, 473, 576
- Garcia-Bellido J., Haugbolle T., 2008, *JCAP*, 0809, 016
- Guy J., Sullivan M., Conley A., Regnault N., Astier P., et al., 2010, *Astron.Astrophys.*, 523, A7
- Hogg D. W., Eisenstein D. J., Blanton M. R., Bahcall N. A., Brinkmann J., et al., 2005, *Astrophys.J.*, 624, 54
- Hunt P., Sarkar S., 2010, *Mon.Not.Roy.Astron.Soc.*, 401, 547
- Jackson J., 2012, *Mon.Not.Roy.Astron.Soc.*, 426, 779
- Keenan R. C., Barger A. J., Cowie L. L., 2013, *Astrophys.J.*, 775, 62
- Komatsu E., et al., 2011, *Astrophys. J. Suppl.*, 192, 18
- Labini F. S., Baryshev Y. V., 2010, *JCAP*, 1006, 021
- Lemaitre G., 1997, *Gen.Rel.Grav.*, 29, 641
- Lewis A., Bridle S., 2002, *Phys. Rev.*, D66, 103511
- Lewis A., Challinor A., Lasenby A., 2000, *Astrophys. J.*, 538, 473
- McCarthy P. J., et al., 2004, *Astrophys. J.*, 614, L9
- Marinoni C., Bel J., Buzzi A., 2012, *JCAP*, 1210, 036
- Marra V., Notari A., 2011, *Class.Quant.Grav.*, 28, 164004
- Marra V., Paakkonen M., 2010, *JCAP*, 1012, 021

- Marra V., Paakkonen M., Valkenburg W., 2013, Mon.Not.Roy.Astron.Soc., 431, 1891
- Moresco M., Cimatti A., Jimenez R., Pozzetti L., Zamorani G., et al., 2012, JCAP, 1208, 006
- Moss A., Zibin J. P., Scott D., 2011, Phys.Rev., D83, 103515
- Nishikawa R., Yoo C.-M., Nakao K.-i., 2012, Phys.Rev., D85, 103511
- Percival W. J., et al., 2010, Mon.Not.Roy.Astron.Soc., 401, 2148
- Riess A. G., Macri L., Casertano S., Lampeitl H., Ferguson H. C., et al., 2011, Astrophys.J., 730, 119
- Romano A. E., Sasaki M., Starobinsky A. A., 2012, Eur.Phys.J., C72, 2242
- Scrimgeour M., Davis T., Blake C., James J. B., Poole G., et al., 2012, Mon.Not.Roy.Astron.Soc., 425, 116
- Shirokoff E., Reichardt C., Shaw L., Millea M., Ade P., et al., 2011, Astrophys.J., 736, 61
- Silk J., 1977, A&A, 59, 53
- Simon J., Verde L., Jimenez R., 2005, Phys. Rev., D71, 123001
- Sinclair B., Davis T. M., Haugbolle T., 2010, Astrophys. J., 718, 1445
- Stern D., Jimenez R., Verde L., Kamionkowski M., Stanford S. A., 2010, JCAP, 1002, 008
- Tolman R. C., 1934, Proc.Nat.Acad.Sci., 20, 169
- Valkenburg W., 2012a, Gen.Rel.Grav., 44, 2449
- Valkenburg W., 2012b, JCAP, 1201, 047
- Wang H., Zhang T.-J., 2012, Astrophys.J., 748, 111
- Zhang P., Stebbins A., 2011, Phys.Rev.Lett., 107, 041301
- Zibin J. P., 2008, Phys. Rev., D78, 043504
- Zibin J. P., Moss A., 2011, Class. Quant. Grav., 28, 164005
- Zumalacarregui M., Garcia-Bellido J., Ruiz-Lapuente P., 2012, JCAP, 1210, 009